Design of Simple Low-Cost Mars Microlander

Tomas Svitek

Stellar Innovations, Inc.
1436 Clover Creek Dr, Longmont CO 80503
303-651-7580, tomas@stin.com

Abstract. *This paper describes the development of a simple low-cost Mars microlander that is matched to the capabilities of the recently-approved Mars Micromission program. This particular microlander design is intended to fill a capability gap between two existing landing systems: the large sophisticated soft landers like Mars Polar Lander and the miniaturized DS-2-class penetrators. This microlander would be able to deliver (in a controlled manner) a small but sophisticated science payload to multiple, exciting but risky landing sites (as an example for our point design, we have used the delivery of the 60% scale Sojourner-class minirover).*

The unique attribute of this design is the maximum exploitation of existing technology that is integrated in a unprecedented-simple lander system configuration. This inherent simplicity results in the system that is simultaneously low-cost and robust (and thus reliable). Two key technologies are employed in the microlander design:

- *small solid rocket propulsion (commercially available) with adequate performance, and*
- *integrated FM-CW radar sensor (also commercially available) that is used as the only guidance sensor.*

.The lander design is intended to be field tested soon in order to maximize the probability of mission success.

Introduction

This microlander was conceived in response to the capabilities of the recently-announced Mars Micromission program. This program aims at developing and deploying a new class of affordable Mars exploration missions. The microlander would be carried to Mars in an entry aeroshell by the micromission probe carrier spacecraft that is launched by Ariane 5 as the piggyback payload. The introduction of the Mars Micromission concept generated many exciting diverse ideas for future Mars exploration that were highlighted in several Mars Micromission science workshops and during the latest Discovery proposal cycle.

This particular microlander design is intended to fill a capability gap between two existing landing systems:

1) A large sophisticated lander like Mars Polar Lander is capable of the precision landing with multiple instruments, and serving as the long-term scientific platform on the surface. But its high recurring cost (over $100M, including a dedicated launch) prevents its proliferation and deployment to high-risk scientifically interesting sites.
2) Highly miniaturized DS-2-type penetrators offer low-cost payload surface delivery, particularly suited for experiments requiring subsurface access. The DS-2 design nicely matches the Mars Micromission concept but its ruggedization requirement due to its 10-30K g's impact shock is an insurmountable obstacle for many sophisticated science payloads, particularly involving mobility.

To fill this performance gap, several alternative designs were proposed in the past, based on various schemes for the parachute deceleration and impact attenuation by crushable materials or air bags. The parachute/air-bag deceleration approach was proven by the Mars Pathfinder mission and by the multiple earlier Russian Mars and Lunar lander missions. It will be used by two upcoming European missions to Mars (Beagle-2 and NetLander), as well.

The difficulty with this approach is scaling down towards the smaller physical size, essential for compatibility with the Mars Micromissions. Additionally, in these landing schemes, the landers impacts the surface in an arbitrary orientation and thus requires some mechanical means for positioning itself the right side up. That further degrades the payload mass allocation for a small micromission lander. Incompatibility of the air-bag landing scheme with the Mars Micromission constraints has been verified by an earlier JPL/CNES study.

Our microlander design would enable the low-cost deployment of relatively sophisticated science payload to multiple sites. These landing sites can be more risky (and thus potentially scientifically more interesting) than would be acceptable for a conventional single lander. The payload options includes payloads with mobility or mechanical components (small rovers, manipulator arm), shock-sensitive instruments (e.g., long-period seismometer), tethered microballoons, etc.

The microlander design is carefully matched to the Mars Micromission ASAP probe carrier requirements and results in the net 30% payload mass fraction. This payload capability corresponds to about the 60%-scale Sojourner-type rover (13 kg mass, 50 cm length) -- as an example.

Additionally, an even smaller version of the microlander is being investigated. This smaller microlander would fit within the DS-2-sized aeroshell (35-cm diameter) and carry about 1 kg payload -- for example, the Martian version of the Muses-CN nanorover. Three or four of these entry probes can be launched on a single Mars Micromission ASAP probe carrier and thus 3-4 nanorovers could be deployed on the Martian surface in one low-cost Mars Micromission. This smaller microlander version will require some technology advances, in contrast to its larger version which employs strictly off-the-shelf technology.

Either lander version, the EDL (entry-descent-landing) sequence preserves DS-2 simplicity by eliminating the requirement for a parachute and any complex deployment mechanisms, inertial sensors and guidance software. The mission profile simplification and testability are essential for this low-cost microlander design.

This microlander design employs the small solid propulsion (with relatively modest performance) for impact deceleration and thrust steering. The streamlined guidance scheme requires only minimalistic electronics and sensor suite. The control algorithm can be implemented in hardware for the maximum robustness. The lander would land a modest science payload at less than 15 m/sec vertical velocity, with the negligible horizontal velocity and less than the 500-g impact shock (with the lander material attenuation).

Our goal is to demonstrate in a credible way that the technology for this low-cost microlander is at the sufficient technological readiness. The unique contribution of this design in an integration of several existing proven low-cost technologies into a new class of surface exploration vehicle. The development will result in a coherent microlander point design to the particular set of realistic requirements.

Technical Description

This microlander is designed to satisfy these specific requirements for Mars Micromission compatibility:

a) total entry mass of less than 40 kg (when deployed from the probe carrier spacecraft),
b) maximum aeroshell diameter of 75 cm,
c) recurring microlander EDL cost of few $M, and
d) flight readiness for the 2005 launch opportunity.

The landing system consists of these key components: propulsion hardware, guidance sensor(s), control electronics, and aeroshell and structure.

Propulsion: The key enabling technology for this design is the recent commercial availability of small solid rocket motors with reasonable performance, resulting from growth of the model rocketry hobby (so called High Power Rocketry). The Isp performance of these motors is respectable (210+ sec), given their small size and ambient-pressure nozzle design, and adequate for the Mars landing. The propellant mass fraction is also acceptable, although it may require some mission unique optimization. The reliability and safety record of this propulsion technology is remarkable. Single motors with over 20 kNs total impulse are available (well beyond our mission requirements of about 7 kNs). The space qualification of this commercial technology is being addressed, with the particular focus on the interplanetary cruise dormancy and the ignitor reliability.

During the initial microlander concept design, both liquid and solid propulsion choices for the microlander propulsion subsystem were investigated. The liquid propulsion would have moderately better payload mass fraction and it would allow the significantly more precise landing and result in the lower impact shock.

Ultimately, the deciding factor for the solid propulsion was its commercial availability and possibility of low-cost testing. Solid propulsion systems on the scale similar to the Mars microlander are routinely built and flown solid – as a hobby! The quick-and-dirty approach to the field testing would not be possible with the conventional liquid propulsion. A small company could never credibly contemplate the design and field-testing of a hydrazine-powered Mars lander but we can make such a claim for our solid-propelled microlander.

Besides the low-cost testing option, the solid-propulsion microlander has an additional advantage of minimizing the launch site operations because no fueling is required. This is potentially a great cost driver in the piggyback launch mode, because of the planetary quarantine requirements of any Mars surface mission. This lander design can be shipped via a commercial carrier to the launch site with its solid rocket motors installed, including ignitors, and in its aeroshell, as long as the grounding plug is installed. Thus, no operations that would violate the planetary quarantine requirements are required at the launch site.

The additional advantage of the solid propulsion is its high thrust that minimizes the powered landing sequence to only about 3 seconds. The short thrust duration results in the minimal altimeter sensor requirements (it has to work only below 500 meters altitude) and eliminates the need for roll control.

Besides the single primary solid-rocket motor for the landing deceleration, the microlander is equipped with a number of much smaller solid motors that are symmetrically distributed around the lander CG and provide the fixed impulse of thrust or torque (depending whether they are fired single or in pairs or triplets).

These small control motors have two functions:

a) coarse attitude control during the main motor firing (by firing as a single) and
b) compensation for the excess terminal velocity or main motor underperformance (by firing in symmetrical groups of two or three).

This proven attitude control approach has been used in multiple missile designs.

The current point design has 48 of these small control motors, each with 30 Ns impulse and thrust duration of <0.4 seconds (literally at the Estes rocket sizes, although that would not be likely our first choice). This particular motor sizing was selected to provide the minimum impulse bit for the attitude control torque, as well as the sufficient extra thrust in the case of the main motor underperformance or the excess aeroshell terminal velocity.

There are several possible vendors for both types of motors (Aerotech, ISP, APS, Kosdon, Dr Rocket, CP Technologies as well as Thiokol, ARC and Alliant).

Our microlander design does not include a parachute. It relies solely on the propulsion to slow the lander from an aerodynamic terminal velocity (around 220 m/sec) to a soft landing. It turns out that for small landers (<100 kg), the additional propellant required to replace the parachute deceleration is less then the mass of the parachute and (more importantly) its deployment mortar mechanism. Eliminating the parachute simplifies the system design, lowers its cost and enables higher-fidelity end-to-end lander testing. However, it creates the challenge of separating the front heat shield (addressed below).

Guidance sensor: The minimalistic guidance package for this lander consists of a single sensor type: FM-CW proximity radar altimeter with three independent beams. The altimeter provides both the altitude (in the FM mode) and the velocity vector information (in the CW mode). The off-nadir sensor mounting at 45 degrees will enable the simultaneous measurement of the vertical and horizontal velocity.

We have performed the broad technology review for the optimum sensor design (i.e., searching for the simplest solution that satisfies the requirements). As a first try, we have picked the small rugged Ka-band FM-CW transceiver MMIC module from M/A-Com (this module is a core sensor for many police radars and is also used in a bomb proximity fuse). Very basic additional electronics is required to complete the radar altimeter: a) triangular wave generator to bias the varactor diode (a simple 555 circuit), b) low-pass filter and Schmidt trigger to convert the radar output signal to the digital signal and c) the set of up/down counters. The radar is equipped with a 20-dB horn antenna.

We are currently performing the bench and field testing of this radar altimeter. This example of adopting simple commonly-available technology for the microlander design is a key attribute of our design approach.

Control electronics: Our baseline design includes a very simple guidance control algorithm. Instead of conventional rocket/missile guidance algorithms, we propose much simpler approach: The thresholding of the matched radar Doppler (CW mode) and distance (FM mode) counters will generate individual firing impulses to the primary and control motors.

The guidance algorithm must correct for these errors:

- dispersion in the microlander terminal velocity (due to the variation in atmospheric density, local altitude or aeroshell ballistic coefficient),
- non-ideal performance of the primary motor,
- misalignment of the primary motor thrust vector,
- horizontal velocity due to winds or entry residuals,
- local terrain slope,
- lander oscillatory motion due to the aeroshell transonic dynamic instability, and
- radar altitude and velocity error.

It turns out that all these error sources can be converted into the adding or subtracting pulses from the FM-CW range/Doppler radar. For example, let's assume that the microlander has a perfect attitude when the main motor fires. In this case, all three radar sensors will measure the same signal and the differential Doppler/range count will be zero. However, due to the thrust misalignment, the microlander now starts to pitch. When that happens, the radar sensor closest to the positive pitch axis will start outputting the lower range count and higher Doppler count – in comparison with the average of the other two sensors. When the pitch angle increases beyond certain value, the Doppler count surplus from the most affected sensor will exceed the other two counters by a predetermined threshold and the register overflow will trigger a control motor firing physically closest to the affected sensor.

Similar analysis can be made for other attitude control disturbances (compensating for the aerodynamic instability, horizontal velocity, and local slope). All these disturbances have similar signature and the lander does not need to know whether it has to fire a certain control motor because its pitch is off or because of the need to compensate for the horizontal ground velocity or for some other reason.

Almost identical control approach can be also used for the landing velocity control. The primary motor will be sized for the maximum motor performance and the minimum terminal velocity. If the landing velocity is too high, in relationship to the range, the small control motors will be fired in a symmetrical configuration to provide additional small impulse. Thus, the worst-case impact velocity of about 40 m/sec (using the main solid motor alone) will be reduced to the worst case impact velocity of about 15 m/sec (using the control motors).

This guidance approach is not the most efficient method and it would not work for the long thrust duration or for the accurate pointing requirements. But it meets the microlander mission requirements, according to our preliminary analysis, and it cannot be matched in its simplicity. Figure 1 shows the results from the preliminary Monte-Carlo 6-DOF simulation.

We have been working on the implementation of this control algorithm for a field-test demonstration. The simple Basic Stamp 2 single-board computer has adequate performance for implementation of this algorithm. For the actual Mars landing hardware, we would implement this algorithm in hardware (FPGA) for the maximum robustness. The expected control rate for the Mars landing is 10-15 Hz.

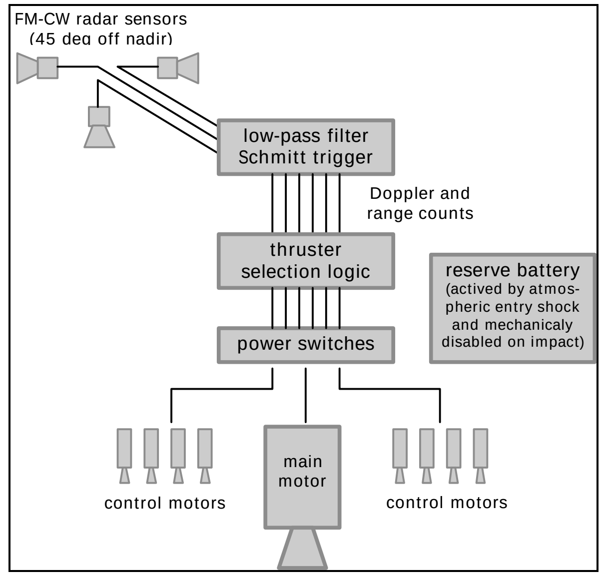

Fig. 2. Microlander Electronics Block Diagram shows the fundamental simplicity of this Mars microlander design

The final component of the microlander electronics is the battery. Our baseline design assumes that the lander electronics will be active for only short time: from the atmospheric interface until the final surface impact. There is no reason for the electronics to be active before the atmospheric entry and we are assuming that lander payload will be self-sufficient and will not require any resources from the EDL electronics.

Typically, planetary entry probes include a G-switch to trigger the EDL sequence. We are proposing to combine the G-switch function with the battery. A proven reserve silver-zinc battery is activated by the shock of the atmospheric entry (>30 Gs). At that point, the microlander electronics is powered on and the radar altimeter starts to search for the surface (the remainder of the landing sequence is described below).

Aeroshell is the critical component of any planetary entry probe. After exploring several possible aeroshell configurations (Pathfinder, DS-2, Stardust and Discoverer, in discussions with JPL, NASA/Langley and several companies), we have adopted the Stardust-shape aeroshell, primarily for its the volume packaging efficiency. The Mars Micromission probe carrier spacecraft can carry the 90%-scaled Stardust aeroshell.

The Stardust aeroshell development experienced difficulties with the aerodynamic dynamic instability in two flight regimes. The hypersonic instability is solved for the microlander mission in a similar way as for Stardust: the preliminary scaling calculation shows that the 6 rpm spin stabilization is adequate for the Mars microlander. This spin rate can be handled by the microlander guidance without requirement for the despin maneuver.

The potential transonic instability of the Stardust aeroshell is mitigated by locating the CG lower in aeroshell (0.29D, instead of 0.35D for Stardust), thus assuring the complete static stability. The aeroshell is still slightly dynamically unstable (as most entry aeroshells are in the transonic regime) but the control system can handle up to 30 deg oscillations when the primary motor is ignited.

The preliminary analysis shows that a conventional ablative heat-shield material will be adequate for this mission. The choices include the proven SLA-561 (from Lockheed-Martin Astronautics) or equivalent materials from Aerotherm (Acusil) or Applied Research Associates (AMRAAM). More advanced materials (SIRCA/PICA) could be also used if justified.

In order to simplify the entry sequence, it is important to maintain (some) RF transparency of the aeroshell for the radar sensors. SLA-561 material has been successfully tested for this purpose. The radar can tolerate up to 12 dB signal of the aeroshell loss.

The cartoons on the previous page show the preliminary structural design of the microlander. The primary loading carrying structure consists of three vertical ribs that runs across the aeroshell. The primary motor is mounted in the ribs intersection (below CG) and the small control motors are attached to the rib sides (4 motors on each side of rib halves, for a total of 48 control motors). The microlander electronics, the battery, and three radar sensor heads are also attached to the ribs.

The science payload is attached to the top of three ribs. The payload CG location is severely constrained and it will have to be as close to the rib top plane, as possible (within about 8 cm). Alternatively, if the higher payload CG location is absolutely required, it will have to be compensated by the aeroshell tip ballast that will reduce the payload mass (approximately 1 kg payload mass penalty per 1 cm CG upward shift).

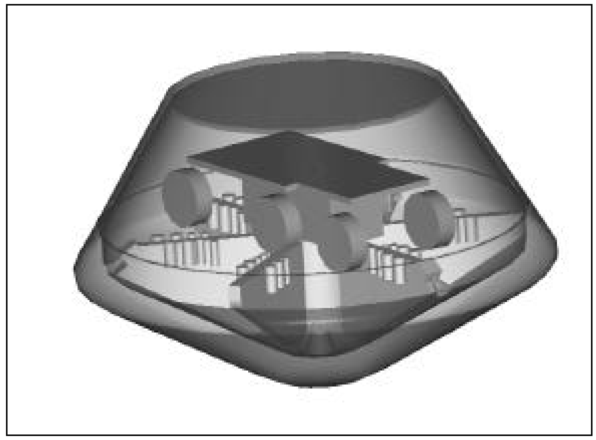

Fig. 3. Microlander proper is located in the bottom half of the Stardust-shaped aeroshell (front shell). Payload (a small rover in this picture) is located in upper half of aeroshell (aft shell). The combined CG location is approximately at mid-point between two shells.

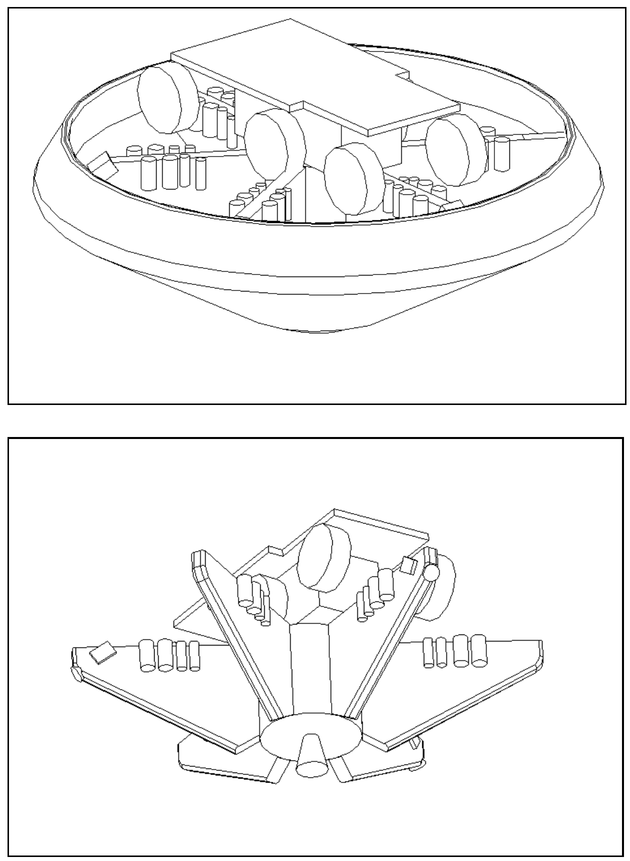

Fig. 4ab. Microlander structure supports main and control motors, guidance sensors, microlander electronics and payload.

Table 1. The preliminary mass budget shows credible 30% payload fraction.

Component	*Estimate [kg]*	*Basis of Estimate*
Total payload	45.0	Mars Micromission RFP allocation
Spacecraft separation system	5.0	JPL Mars Micromission team estimate
Entry probe	40.0	
Front heat shield ablator	3.0	material mass scaled from similar entry probes
Front aeroshell substrate	1.5	estimated honeycomb mass
Aft heat shield ablator	1.2	material mass scaled from similar entry probes
Aft aeroshell substrate	0.7	estimated honeycomb mass
Aeroshell separation mechanism	0.4	paraffin actuator
Deployment guides (3)	0.6	estimated aluminum machined guides
Aeroshell total	7.4	
Microlander allocation	32.6	includes surface science payload
Main motor propellant	3.3	7,200 Ns
Main motor case	2.1	60% propellant mass fraction
Main motor mounting	0.4	machined bracket
Main motor ignitor	0.1	estimate
Control motors propellant (48)	0.8	30 Ns each
Control motors cases	1.2	40% propellant mass fraction
Control motors mounting	0.4	straps
Propulsion subtotal	8.3	
FM-CW radar sensors (3)	0.9	incl. small horn antenna and aux electronics
Control electronics	0.3	
Propulsion drivers	0.4	electric power switches for ignitors
Reserve battery	0.2	<1 Wh capacity, 2 A/5 V instant current ability
Impact disabling switch	0.1	
Electrical harness	0.5	
Electronics total	2.4	
Structural ribs (3)	2.4	composite honeycomb panels
Impact absorption	1.0	material (rib bottom for impact shock damper)
Payload attachment (3)	0.9	machined brackets
Thermal protection	0.5	protection against initial main motor firing
Structure subtotal	4.8	
Microlander subtotal	15.5	includes propulsion, electronics and structure
Microlander reserve	4.0	
Total microlander	19.5	
Surface payload allocation	13.1	corresponds to 60%-scaled Sojourner rover

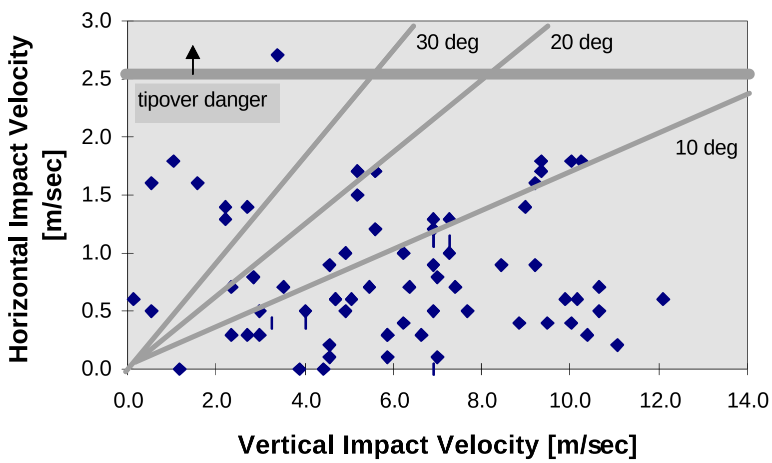

Fig. 5. Preliminary results of 6-DOF Monte-Carlo simulations shows the surface impact vertical and horizontal velocities are within the expected range.

Landing Sequence

The landing sequence consists of the following events (cartoons in the right column correspond to the text paragraphs in the column below):

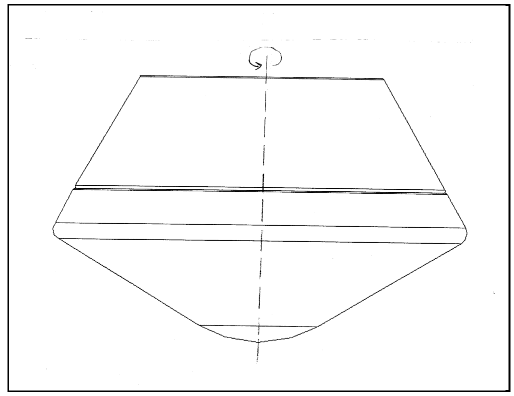

1) *Entry probe separation* from the probe carrier spacecraft occurs 1-5 days before the entry. Probe is inert during the cruise.

2) *Atmospheric interface* of the spin-stabilized probe. The entry shock activates the microlander reserve battery. The radar starts to operate and is looking for the surface echo.

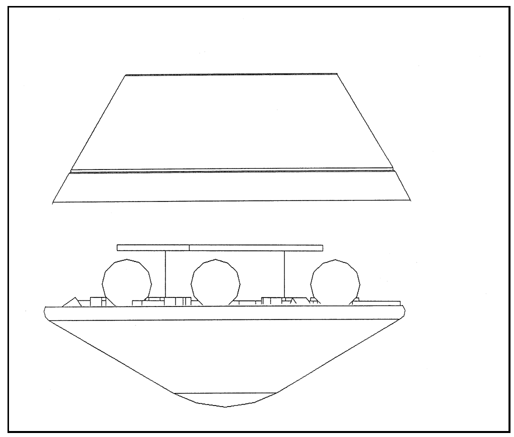

3) *Aft aeroshell separation* at 2-3 minutes after the atmospheric entry. The conventional lander designs typically employ the G-switch/timer and the electronically activated separation pyro-mechanism. Our baseline design is passive: it uses a single non-explosive paraffin actuator that is activated simply by the propagating thermal wave through the aft aeroshell. The idea requires careful modeling and testing of the local thermal design of the paraffin actuator but it is more reliable. Aerodynamic forces will separate the aft aeroshell from the remaining entry probe (aft aeroshell will slide on three guides to protect the microlander payload from recontact).

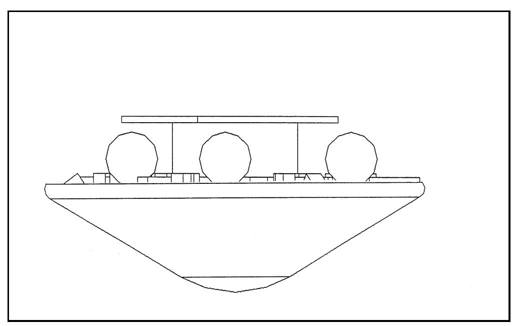

4) During *the remainder of the descent* through the transonic regime, microlander is going at its terminal velocity (210-250 m/sec), and it will pick up some oscillatory motion. The radar is searching for the reflected surface signal.

5) *Radar signal is acquired* at about 500-700 m above the surface. The microlander is waiting for the preset altitude (around 350 m) to activate the control electronics.

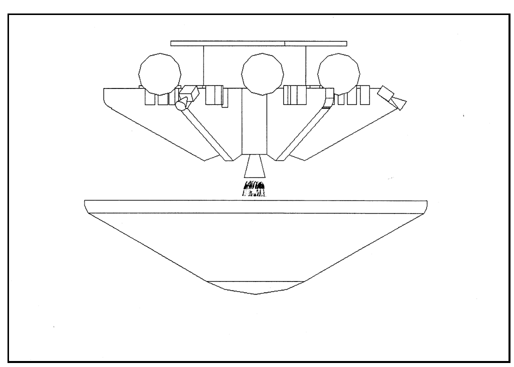

6) *Primary motor is ignited* while the lander is still descending in the front aeroshell. The design envisions that the microlander (with the attached payload) will `fly away' from the front shell (as if the microlander would be sitting on the surface and the front aeroshell would be used as a launch pad). This approach requires additional mass for Nomex thermal protection of the microlander and its payload but it is, by far, the simplest approach.

7) *Primary and control motors* are firing during the remaining 3 seconds of the powered flight. Nominally (i.e., the worst-case motor underperformance), the primary motor would stop firing just before the surface contact. There is always some residual thrust tail-off for the next 1-2 seconds but it does not create sufficient thrust to effect the landing impact dynamics. However, in the worst-case (i.e., the primary motor overperformance), the control lander will come to a stop at about 15 meters above the surface and it will free fall for another <3 seconds with the terminal impact velocity under 10 m/sec (the small control motors are still providing the attitude control and possibly additional deceleration thrust).

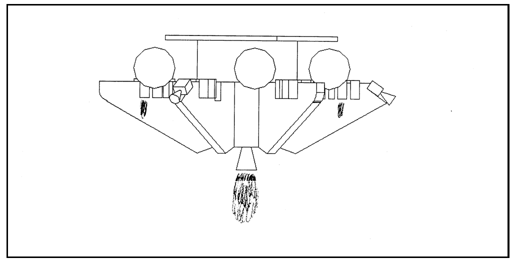

8) *The microlander impacts the surface*. Some of the impact shock is absorbed by the microlander structure. The microlander structural ribs are made from the crushable material and the primary motor nozzle can collapse inside the motor chamber. This microlander impact shock absorption limits the payload impact shock to under 500 Gs. The surface impact also inhibits (by interrupting the battery power) the microlander electronics so additional control motor firings are disabled.

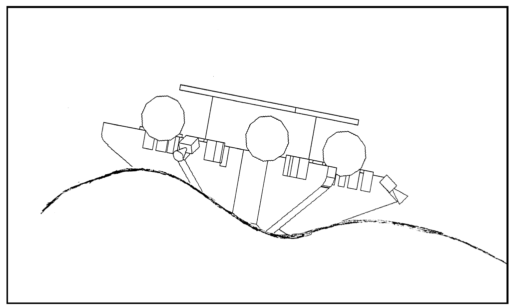

9) *The lander payload is activated* and starts its nominal function. As an example, the minirover depicted in illustrations would simply drive away at this time, from the microlander impact site. It is assumed that any EDL telemetry will be stored and relayed by the payload. It would be relatively straightforward to equip the microlander electronics with a dedicated telemetry buffer and the UHF Proximity-1 transceiver, but these functions have to be implemented in the science payload, anyway. Not duplicating these functions is optimum for this mass constrained system.

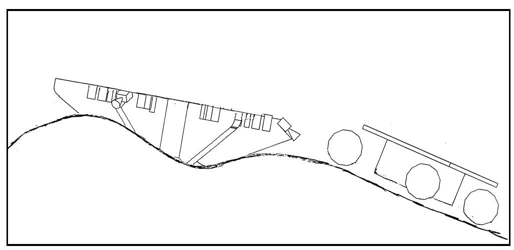

Tipover analysis: One of the primary advantages of this microlander design is its ability to land the right side up (in contrast to airbag landers). The need for the relatively massive mechanism for turning the lander over, after the impact, is thus eliminated. However, this benefit comes at a risk – if this microlander would tipover during the landing sequence, its mission would be over. We have attempted to calculate probability of the lander tipover. Tipover can happen for two reasons or their mutual combination:

a) if one edge of the lander hits the rock and the other lander edge lands in the soft soil, the lander is tilted and it could fall over, or

b) if the residual horizontal velocity is above certain threshold (2 m/sec) and is comparable to the vertical velocity (for that reason, we would never want to land with the exactly zero vertical velocity).

The lander tipover becomes plausible when the size of a rock it hits exceeds about 40 cm. Based on the Viking and Pathfinder site analysis, the probability of hitting such a rock is less than 5%. The probability of excessive horizontal velocity, based on the preliminary Monte-Carlo 6-DOF simulation, also appears to be also much less than 5%. The tipover probability from the combined effects (larger rocks and substantial residual horizontal velocity) remains to be analyzed.

Current Status: Stellar has been developing this microlander concept, in cooperation with its partners, for the past two years, using the company R&D funding. So far, we have received positive feedback to our design, both from the prospective users (scientific investigators) and sponsors (funding agencies), but no flight hardware commitment is imminent.

The photos on the right show the functional breadboard of the microlander (with only one radar sensor and scaled-down propulsion for the terrestrial terminal velocity). Our intention is to upgrade the microlander breadboard with the full sensor and motor complement and start field testing of the design.

The field testing will be done initially by raising the microlander to about 200 meter altitude with a small balloon. The next microlander design iteration would be drop tested at an established instrumented test range (most likely, Navy China Lake Air Warfare Station), if the government sponsor is found.

Mars Ascent Vehicle synergy: The obvious on-going effort that is technologically related to the described microlander design is the MAV development by JPL and the industry partners. This microlander concept was developed independently from MAV, but there are clearly some obvious synergies. However, MAV is a component of the international highly-visible program and thus cannot fail. In contrast, this microlander design is offered in the true spirit of the low-cost failure-is-acceptable-if-it-advances-technology (consistent with the Mars Micromission concept). There is an obvious threat of rapidly escalating microlander costs if it is integrated too tightly with the MAV development and its requirements. The expensive solid-propelled microlander is not attractive. At that point, the conventional liquid-propulsion lander simply becomes more attractive.

Other mission options: The Mars Micromission mission mode was used as a starting point for developing the point design, to establish feasibility and utility of the piggyback-launched microlander technology. However, this microlander design could be also launched in different ways, and deployed to different targets that have a similar landing requirements (specifically, Moon, Phobos, Mercury or Europa).

Acknowledgments: This design is only possible because of the previous incredible and multi-faceted R&D efforts by many individuals, aimed at developing miniaturized space technologies as well as because of the spin-off technologies from other fields.

The described effort is a synthesis of these advances into a credible integrated microlander system design. We would like to appreciate the useful discussions, assistance with information and encouragements by many individuals. Specifically, we would like to mention Jeff Zerr, Pavel Svitek, Bruce Murray, Jim Cutts, Mike Malin, Rob Manning, Doug Stetson, Ross Jones, George Powell, Eric Slimko, Sarah Gavit, Gil Moore, Mike Larra, Gordon Hardman, Jan King, Jim Burke, John Wickman, John Whitehead, Bill Martin, Robert Mitcheltree, and Bill Willcockson.

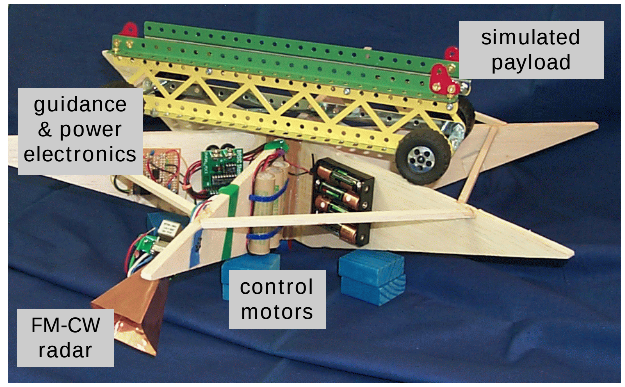

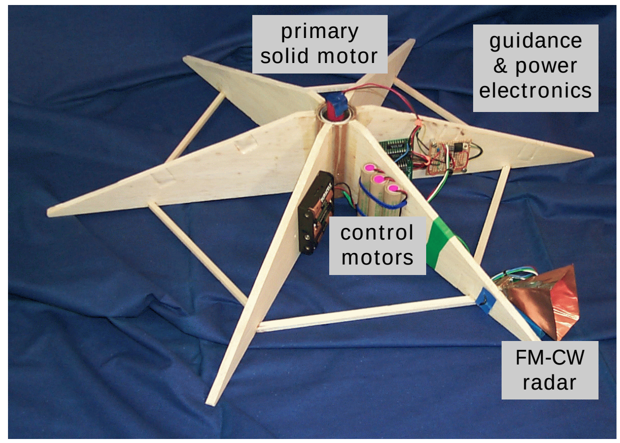

Fig. 6ab. Functional Microlander breadboard is intended for benchtop testing. It will be soon upgraded with full complement of sensors and motors and field tested. The upper photo shows the simulated payload. The microlander is inverted in the lower photo to show primary motor (scaled for terrestrial terminal velocity).